CLNS 05/1907
CLEO 05-2

Limits on Neutral D Mixing in Semileptonic Decays

C. Cawlfield,[1] B. I. Eisenstein,[1] G. D. Gollin,[1] I. Karliner,[1] D. Kim,[1] N. Lowrey,[1] P. Naik,[1] C. Sedlack,[1] M. Selen,[1] J. Williams,[1] J. Wiss,[1] K. W. Edwards,[2] D. Besson,[3] T. K. Pedlar,[4] D. Cronin-Hennessy,[5] K. Y. Gao,[5] D. T. Gong,[5] Y. Kubota,[5] T. Klein,[5] B. W. Lang,[5] S. Z. Li,[5] R. Poling,[5] A. W. Scott,[5] A. Smith,[5] S. Dobbs,[6] Z. Metreveli,[6] K. K. Seth,[6] A. Tomaradze,[6] P. Zweber,[6] J. Ernst,[7] A. H. Mahmood,[7] K. Arms,[8] K. K. Gan,[8] H. Severini,[9] D. M. Asner,[10] S. A. Dytman,[10] W. Love,[10] S. Mehrabyan,[10] J. A. Mueller,[10] V. Savinov,[10] Z. Li,[11] A. Lopez,[11] H. Mendez,[11] J. Ramirez,[11] G. S. Huang,[12] D. H. Miller,[12] V. Pavlunin,[12] B. Sanghi,[12] E. I. Shibata,[12] I. P. J. Shipsey,[12] G. S. Adams,[13] M. Chasse,[13] M. Cravey,[13] J. P. Cummings,[13] I. Danko,[13] J. Napolitano,[13] Q. He,[14] H. Muramatsu,[14] C. S. Park,[14] W. Park,[14] E. H. Thorndike,[14] T. E. Coan,[15] Y. S. Gao,[15] F. Liu,[15] R. Stroynowski,[15] M. Artuso,[16] C. Boulahouache,[16] S. Blusk,[16] J. Butt,[16] E. Dambasuren,[16] O. Dorjkhaidav,[16] J. Li,[16] N. Menaa,[16] R. Mountain,[16] R. Nandakumar,[16] R. Redjimi,[16] R. Sia,[16] T. Skwarnicki,[16] S. Stone,[16] J. C. Wang,[16] K. Zhang,[16] S. E. Csorna,[17] G. Bonvicini,[18] D. Cinabro,[18] M. Dubrovin,[18] S. McGee,[18] A. Bornheim,[19] S. P. Pappas,[19] A. J. Weinstein,[19] H. N. Nelson,[20] R. A. Briere,[21] G. P. Chen,[21] J. Chen,[21] T. Ferguson,[21] G. Tatishvili,[21] H. Vogel,[21] M. E. Watkins,[21] J. L. Rosner,[22] N. E. Adam,[23] J. P. Alexander,[23] K. Berkelman,[23] D. G. Cassel,[23] V. Crede,[23] J. E. Duboscq,[23] K. M. Ecklund,[23] R. Ehrlich,[23] L. Fields,[23] L. Gibbons,[23] B. Gittelman,[23] R. Gray,[23] S. W. Gray,[23] D. L. Hartill,[23] B. K. Heltsley,[23] D. Hertz,[23] L. Hsu,[23] C. D. Jones,[23] J. Kandaswamy,[23] D. L. Kreinick,[23] V. E. Kuznetsov,[23] H. Mahlke-Krüger,[23] T. O. Meyer,[23] P. U. E. Onyisi,[23] J. R. Patterson,[23] D. Peterson,[23] J. Pivarski,[23] D. Riley,[23] A. Ryd,[23] A. J. Sadoff,[23] H. Schwarthoff,[23] M. R. Shepherd,[23] S. Stroiney,[23] W. M. Sun,[23] D. Urner,[23] T. Wilksen,[23] M. Weinberger,[23] S. B. Athar,[24] P. Avery,[24] L. Breva-Newell,[24] R. Patel,[24] V. Potlia,[24] H. Stoeck,[24] J. Yelton,[24] and P. Rubin[25]

(CLEO Collaboration)

[1] *University of Illinois, Urbana-Champaign, Illinois 61801*
[2] *Carleton University, Ottawa, Ontario, Canada K1S 5B6 and the Institute of Particle Physics, Canada*
[3] *University of Kansas, Lawrence, Kansas 66045*
[4] *Luther College, Decorah, Iowa 52101*
[5] *University of Minnesota, Minneapolis, Minnesota 55455*
[6] *Northwestern University, Evanston, Illinois 60208*
[7] *State University of New York at Albany, Albany, New York 12222*
[8] *Ohio State University, Columbus, Ohio 43210*
[9] *University of Oklahoma, Norman, Oklahoma 73019*
[10] *University of Pittsburgh, Pittsburgh, Pennsylvania 15260*
[11] *University of Puerto Rico, Mayaguez, Puerto Rico 00681*
[12] *Purdue University, West Lafayette, Indiana 47907*
[13] *Rensselaer Polytechnic Institute, Troy, New York 12180*
[14] *University of Rochester, Rochester, New York 14627*
[15] *Southern Methodist University, Dallas, Texas 75275*
[16] *Syracuse University, Syracuse, New York 13244*
[17] *Vanderbilt University, Nashville, Tennessee 37235*

[18]*Wayne State University, Detroit, Michigan 48202*
[19]*California Institute of Technology, Pasadena, California 91125*
[20]*University of California, Santa Barbara, California 93106*
[21]*Carnegie Mellon University, Pittsburgh, Pennsylvania 15213*
[22]*Enrico Fermi Institute, University of Chicago, Chicago, Illinois 60637*
[23]*Cornell University, Ithaca, New York 14853*
[24]*University of Florida, Gainesville, Florida 32611*
[25]*George Mason University, Fairfax, Virginia 22030*
(Dated: February 5, 2005)

Abstract

Using the CLEO II.V detector observing e^+e^- collisions at around 10.6 GeV we search for neutral D mixing in semileptonic D^0 decays tagged in charged D^* decays. Combining the results from the $Ke\nu$ and $K^*e\nu$ channels we find that the rate for D mixing is less than 0.0078 at 90% C.L.

The study of mixing in the K^0 and B_d^0 sectors has provided a wealth of information to guide the form and content of the Standard Model. In the framework of the Standard Model, mixing in the charm meson sector is predicted to be small [1], making this an excellent place to search for non-Standard Model effects.

A D^0 can evolve into a $\overline{D^0}$ through well known, on-shell intermediate states, or through off-shell intermediate states such as those that might be present due to new physics. We denote the amplitude through the former (latter) states by $-iy$ (x), in units of $\Gamma_{D^0}/2$ [2]. The Standard Model contributions to x are suppressed to $|x| \approx \tan^2\theta_C \approx 5\%$ and the Glashow-Illiopolous-Maiani [3] cancellation could further suppress $|x|$ down to $10^{-6} - 10^{-2}$. Many non-Standard Model processes could lead to $|x| > 1\%$. Signatures of new physics include $|x| \gg |y|$ and CP violating interference between x and y or between x and a direct decay amplitude.

Observation of D mixing in hadronic decay channels is complicated by doubly Cabibbo suppressed decays, where both the decay of the original charm quark and subsequent charged W decay proceed in Cabibbo suppressed modes. Such a decay mimics mixing of a D^0 to a $\overline{D^0}$ followed by the dominant Cabibbo allowed channel decay. In semileptonic decays no such double suppression is allowed as the W decays to a charged lepton and neutrino, and the charge of the lepton tags whether a c, producing a positive lepton, or $\bar{c}$, producing a negative lepton, has decayed. When the production flavor of the D is tagged in charged D^* decay or some other way, a wrong sign lepton produced in a subsequent semileptonic decay unambiguously signals D mixing. Other mechanisms that produce leptons of the opposite sign in D^0 or $\overline{D^0}$ decay are highly suppressed. The integrated mixing rate normalized to the total decay rate is equal to $\frac{1}{2}(x^2 + y^2)$, and is called R_M. This is at once good and bad news. The observation of any wrong sign semileptonic D decay is an unambiguous signal of D mixing. With both x and y small ($< \mathcal{O}(0.01)$) the rate of wrong sign semileptonic D decays will be very small ($< \mathcal{O}(0.0001)$), and an observation of D mixing in semileptonic decays would not give insight on the relative sizes of x and y. In contrast hadronic decays have wrong sign contributions from both doubly Cabibbo suppressed decays and mixing. The two channels interfere resulting in a term that depends on a linear combination of x and y, and the proper time dependence of wrong sign final states can be used to measure x and y separately.

The proper decay time dependence of semileptonic mixed final states in units of the mean D^0 lifetime, $t_{D^0} = (410.3 \pm 1.5)$fs [4], is $r(t) \equiv (x^2+y^2)t^2e^{-t}$. Thus mixed semileptonic decays should populate larger proper times with an average decay time of three. The dominant direct decays are distributed as e^{-t} with an average decay time of one. This difference is taken advantage of to increase the sensitivity to D mixing.

To date no one has observed evidence for D mixing in any channel. The best limit on R_M comes from the FOCUS collaboration [5] where they find $R_M < 0.0010$ at 90% C.L. Belle [6] reports a similar limit, $R_M < 0.0014$ at 90% C.L. and BABAR [7] a higher limit of $R_M < 0.0042$ at 90% C.L. Other limits on D mixing are summarized in [8]. Our experimental situation is very similar to Belle and BABAR, but our data sample is more than an order of magnitude smaller. Thus we expect not to be sensitive to any D mixing signal and set limits higher than above.

Our data were collected using the CLEO II.V upgrade [9] of the CLEO II detector [10] between February 1996 and February 1999 at the Cornell Electron Storage Ring (CESR). The data correspond to 9.0 fb^{-1} of e^+e^- collisions near $\sqrt{s} \approx 10.6$ GeV. The detector consisted of cylindrical tracking chambers and an electro-magnetic calorimeter immersed in a 1.5 Tesla axial magnetic field, surrounded by muon chambers. The reconstruction of displaced vertices from charm decays is made possible by the addition of a silicon vertex detector (SVX) in CLEO II.V. The charged particle trajectories are fit using a Kalman filter technique [11] that takes into account energy loss as the particles pass through the material of the beam pipe and detector. Specific ionization for charged particle identification is measured in the main drift chamber with a resolution of about 7%. Electrons above 500 MeV/c momentum are also identified by matching of track momentum with calorimeter energy deposition and requiring that the calorimeter shower has the characteristics expected of an electro-magnetic rather than a hadronic shower. Hadrons are misidentified as electrons at roughly the 0.1% level from studies of known hadron samples in the data. Muons are not used as the CLEO muon identification system cannot cleanly identify muons below about 1.5 GeV/c momentum and the small sample of clean muons are not useful to study semileptonic D decays at our beam energy.

To study backgrounds and relative selection efficiencies we use a GEANT [12] based detector simulation of our data. We use simulations of $e^+e^- \to q\bar{q}$ with the quarks fragmenting and particles decaying generically guided by previous measurements. The data of this generic simulation corresponds to roughly ten times the luminosity collected by the detector. We also use simulations of $e^+e^- \to \tau^+\tau^-$ and $e^+e^- \to B\overline{B}$ to study small contributions to the background. For these studies the simulated samples are reconstructed and selected using the same methods as the data sample as described below.

To select hadronic events and ensure that the event production point is well known there must be at least five well reconstructed tracks consistent with coming from the interaction region. The tracks must carry more than 15% of the collision energy. This selection is nearly 100% efficient, removes events that would not pass subsequent reconstruction requirements, and ensures a well measured D^0 flight distance. All tracks used in the reconstruction of the decay chain except the pion from the charged D^* decay are required to hit at least two of the three SVX planes in projections both transverse and parallel to the beam direction.

The D^0s are tagged at production in the decay of the charged D^* to a charged pion and a D^0. A π^+ indicates that a D^0 has been produced and a π^-, a $\overline{D^0}$. Subsequent direct semileptonic decays of the D^0 or $\overline{D^0}$ produce a charged lepton of the same sign as the pion from the D^* decay, called right sign (RS) combinations, while semileptonic D decay after mixing produces a charged lepton of the opposite sign, called wrong sign (WS) combinations. Since little energy is released in the D^* decay the pion is limited to a momentum of 400 MeV/c at our beam energy, and is called the soft pion. We choose combinations such that the momentum of the D^0 is larger than 2.0 GeV/c and thus are dominated by D^0s produced in $e^+e^- \to c\bar{c}$ with only a small contribution produced by B decays. The analyses find RS combinations maximizing the signal to noise for the decay chains $D^* \to \pi_{\rm soft} D^0 \to K^{(*)} e\nu$. The same selections are then used to find WS combinations, and the ratio of WS to RS combinations after accounting for background is a measure of R_M. The analysis of the $D^0 \to Ke\nu$ channel is described in full detail in [13] while the $D^0 \to K^* e\nu$ channel is similarly described in [14].

The $D^0 \to Ke\nu$ analysis uses a neural net to distinguish signal events from background. All combinations of electrons, kaons identified loosely via specific ionization, and $\pi_{\rm soft}$ are considered. Eighteen variables are inputs to the net. They are selected such that our simulation describes their distribution well, and in general they describe the kinematics of the $\pi_{\rm soft}$, kaon, and electron candidates separating random combinations from those produced in the desired decay chain. For example one input is the cosine of the angle between the

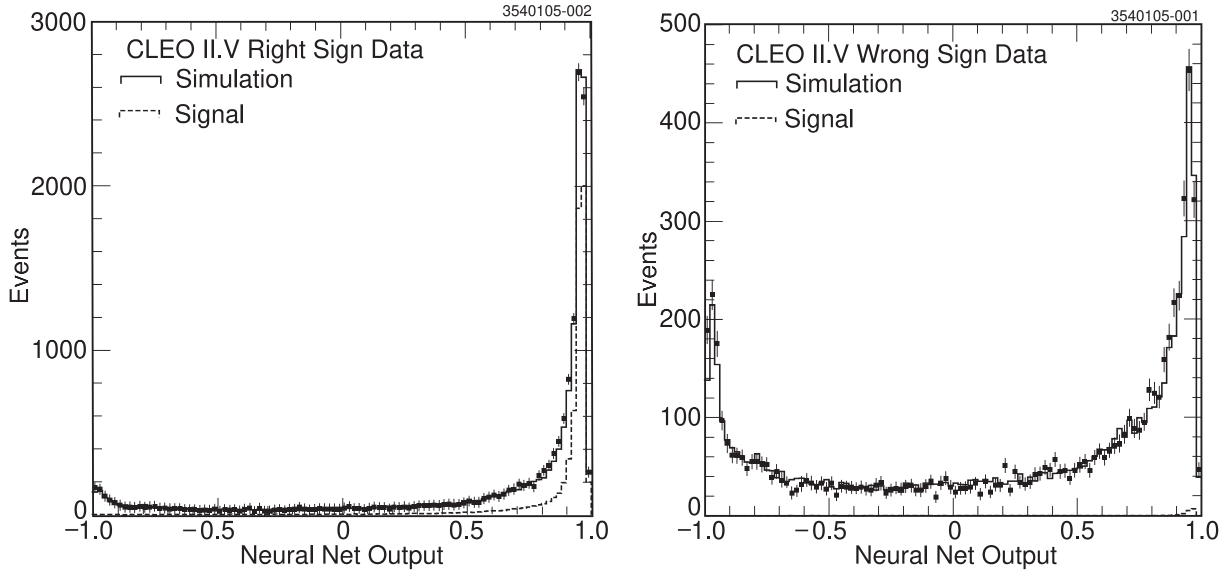

FIG. 1: The output of the neural net used in the $D^0 \to Ke\nu$ analysis for the RS (left) and WS (right) samples comparing data (squares) with simulation (full histogram). Also shown with a dashed histogram is the predicted contribution of the signal. The very small WS signal is at the central value found by this analysis.

electron and the kaon which peaks near one for the signal and at both one and negative one for background. The net is trained on our simulation and produces an output near one for signal-like combinations and negative one for background-like combinations. Figure 1 shows the output of the neural net on RS and WS candidates. According to the simulation the RS sample is roughly 42% signal while we expect the WS to be dominated by background. We compare the output of the neural net thoroughly with the prediction of the simulation by varying both its input and structure. The simulation is found to predict very well changes observed in the data. Combinations with a neural net output of greater than 0.95 are selected for further analysis.

To measure the decay time of the D^0 we refit the tracks requiring that the kaon and electron come from a common D^0 decay vertex, use the thrust axis of the event as the direction of the D^0, and require that the D^0 and $\pi^+_{\rm slow}$ or $\overline{D^0}$ and $\pi^-_{\rm slow}$, come from a common vertex constrained to be in luminous region. This procedure improves the resolution on the decay time by 30% to about half a D^0 lifetime. Figure 2 shows the distribution of the decay times for the RS and WS samples. Overlaid are fits to a signal plus backgrounds. Background shapes are taken from the simulation and are dominated by non-charm events with a significant fraction of non-signal charm decays. The RS distribution is dominated by signal, while the WS is consistent with no signal and thus is dominated by background. Signal shapes are also taken from the simulation. The agreement between data and simulation is good and the normalizations for the RS signal and the background in both the RS and WS distributions agree with the predictions of the simulation.

These fits find 2840$\pm$300 RS signal and 31$\pm$21 WS signal combinations. In the $D^0 \to Ke\nu$ channel we measure $R_M = 0.0110 \pm 0.0076$ and see no evidence for mixing. Systematic uncertainties are discussed below.

The $D^0 \to K^* e\nu$ analysis uses a more traditional approach. The charged K^* is recon-

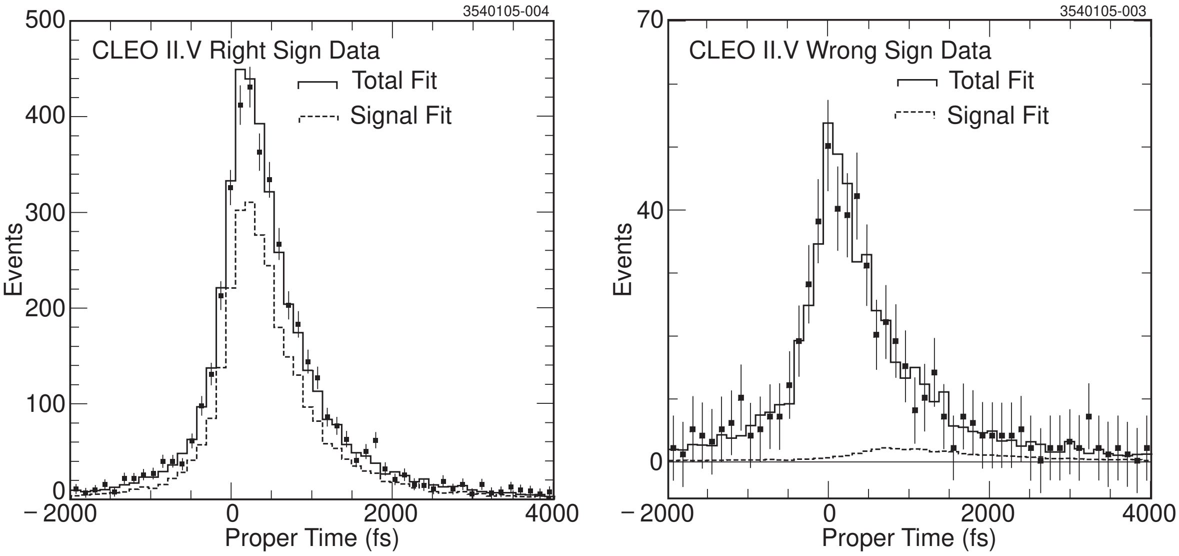

FIG. 2: The decay time for the $D^0 \to Ke\nu$ analysis for the RS (left) and WS (right) samples. The squares show the data, the full histogram shows the fits, and the dashed histogram the signal contribution to the fits.

structed in the $K^0_S\pi$ channel followed by the K^0_S decay to two charged pions. These two pions are fit to a common vertex and the mass of the $\pi\pi$ must be within 16 MeV/c^2 of the expected K^0_S mass. Similarly for the K^*, the K^0_S-π combination must be within 60 MeV/c^2 of the known mass. When the K^* is combined with an electron, and the pair is consistent with coming from a D^0 decay, the sample is fairly clean. The direction of the D^0 is determined with a weighted average of the thrust, the $\pi_{\rm soft}$, and K^*-electron combination directions. This gives a better estimate of the energy release, Q, in the D^* decay and signal is distinguished from background in a fit to the two dimensional Q versus decay time distribution. The decay time is improved by a refit similar to the one described above.

Figures 3 and 4 show the projections of the two dimensional fits on the Q and decay time axes for RS and WS candidates respectively. Shapes for signal and background are taken from the simulation. Agreement between the data and simulation is good both in the signal dominated RS sample and the background dominated WS sample. The prediction of the simulation is checked using $D^* \to \pi_{\rm slow} D^0 \to K^0_S\pi\pi\pi^0$ decays found in the data. The π^0 is ignored and the same methods are applied as in the $K^*e\nu$ analysis to reconstruct a two dimensional Q and decay time distribution. The simulation and the data agree very well in this check sample. The simulation also accurately predicts the size of the observed signal and background in both the RS and WS samples.

These fits find 638$\pm$51 RS signal and -30 ± 8 WS signal combinations. When constrained to find at least zero WS signal the fit returns 0$\pm$2 WS signal combinations. The two results yield similar upper limits on R_M, and the latter is used to combine with the $Ke\nu$ channel as it yields a slightly more conservative upper limit. In the $D^0 \to K^*e\nu$ channel we measure $R_M = 0.0000\pm0.0031$ and see no evidence for mixing. Systematic uncertainties are discussed below.

The two analyses are statistically independent and consistent; therefore they can be combined. We combine their central values weighting by their statistical uncertainties to find $R_M = 0.0016 \pm 0.0029$.

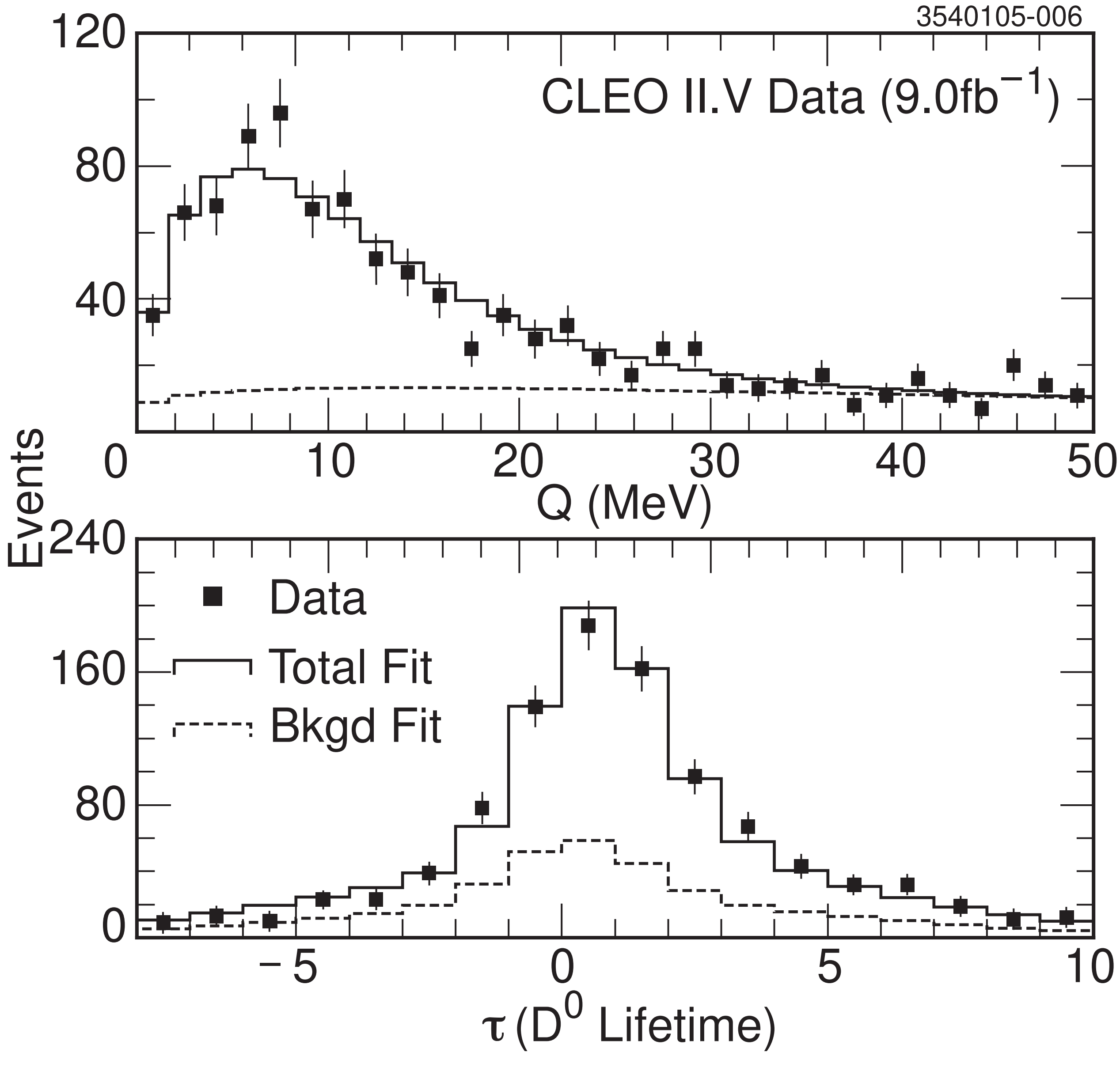

FIG. 3: The Q (top) and decay time (bottom) distributions for the $D^0 \to K^* e\nu$ analysis for the RS sample. The squares show the data, the histograms show projections of the two dimensional fit, and the dashed histogram shows the background contribution to the fit.

The two analyses share some common systematic uncertainties. They both use the same simulation to model backgrounds and signal shapes. We take the smaller of the two systematic uncertainties as the uncertainty on the combined value. The statistical uncertainty on simulated signal and background shapes causes an uncertainty of ± 0.0023 on R_M in the $K^* e\nu$ analysis and ± 0.0028 in the $Ke\nu$ analysis. The shape of the background in the decay time is parametrized from the simulation in a similar way in both analyses. Variations in this parameterization affect the number of RS and WS signal combinations. This variation causes an uncertainty of ± 0.0014 on R_M in the $Ke\nu$ analysis and ± 0.0018 in the $K^* e\nu$ analysis. The lower of the two uncertainties, the first in each case, is taken as the uncertainty

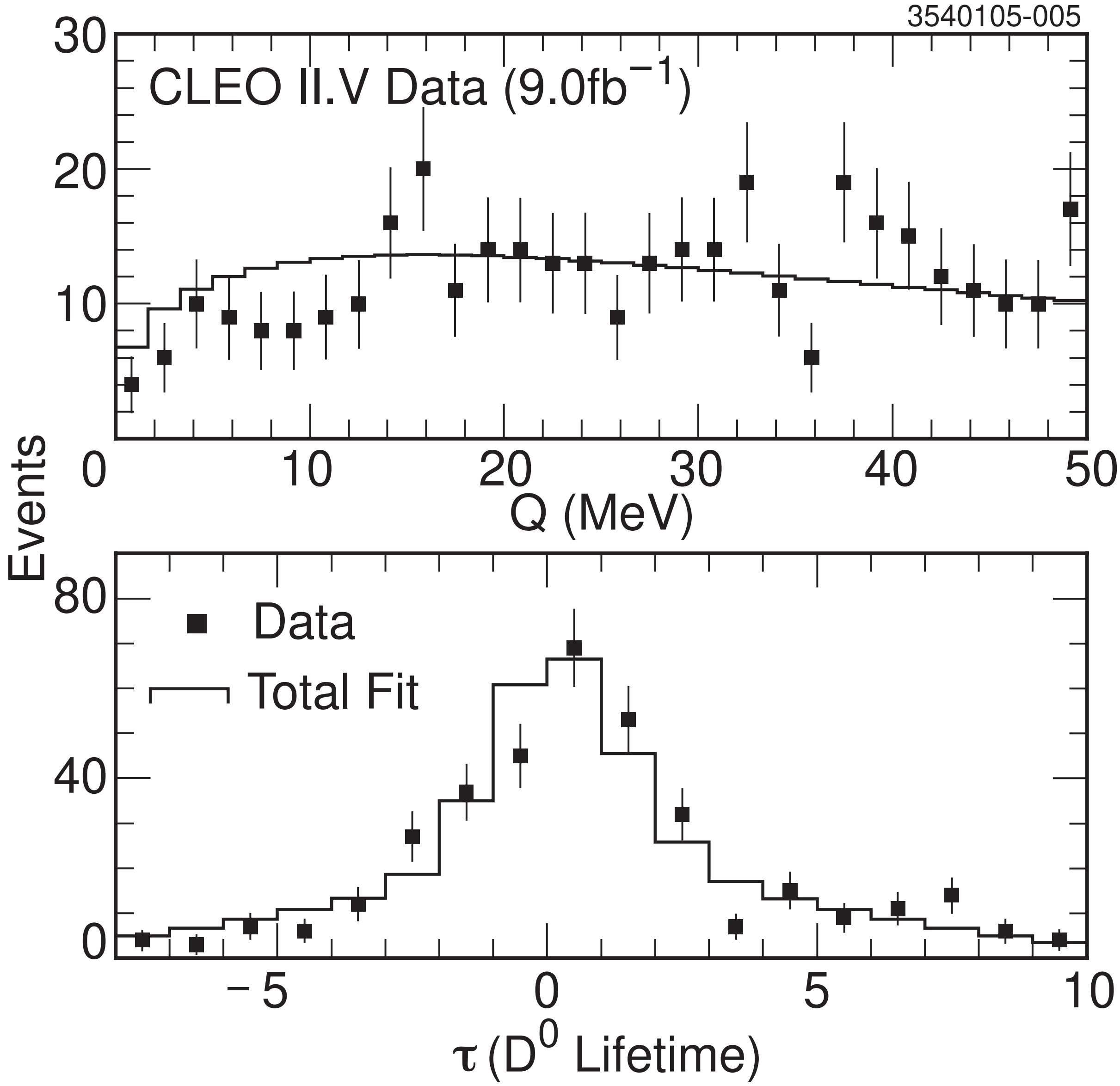

FIG. 4: The Q (top) and decay time (bottom) distributions for the $D^0 \to K^* e\nu$ analysis for the WS sample. The squares shows the data and the histograms shows projections of the two dimensional fit.

on the combined result.

For systematic uncertainties not shared by the two analyses we add them by weighting their contribution to the central value. Specifically uncertainties in the $Ke\nu$ analysis contribute 15% of their size to the combined analysis, while uncertainties in the $K^*e\nu$ analysis contribute 85% of their size. In the $K^*e\nu$ analysis variations of the parametrization of the Q shape for signal and background add ± 0.0008. In the $Ke\nu$ analysis the largest contribution to the uncertainty comes from variations in the electron identification and add ± 0.0007 to the combined result. Details of the lifetime fit (binning, fit range, and D^0 direction choice) add ± 0.0004. Variations in particle identification selections and details of the refit procedure add ± 0.0004. Other systematic effects are studied and found to be negligible.

TABLE I: Summary of uncertainties on R_M.

Source	Size
Statistics	± 0.0029
Simulation Statistics	± 0.0023
Decay Time Shape	± 0.0014
Q Parameterization	± 0.0008
Electron Identification	± 0.0007
Decay Time Fit Details	± 0.0004
Particle ID and Refit Details	± 0.0004
Systematic Total	± 0.0029

All the systematic uncertainties are combined in quadrature to yield a total systematic uncertainty of ± 0.0029. All of the uncertainties are summarized in Table I.

We see no sign of D mixing in either channel and set limits on R_M based on our central value of $0.0016 \pm 0.0029 \pm 0.0029$ where the statistical and systematic uncertainties are combined quadratically. We assume the uncertainty follows a Gaussian distribution and exclude the unphysical region, $R_M < 0$. This gives $R_M < 0.0078$ at 90% C.L. and $R_M < 0.0091$ at 95% C.L. We agree with previous measurements and set limits as expected given the size of our data sample.

We gratefully acknowledge the effort of the CESR staff in providing us with excellent luminosity and running conditions. This work was supported by the National Science Foundation and the U.S. Department of Energy.

---

[1] A.A. Petrov, eConf **C030603** MEC05 (2003) (hep-ph/0311731); H.N. Nelson, hep-ex/9908021.
[2] T.D. Lee, R. Oehme, and C.N. Yang, Phys. Rev. **106**, 340 (1957); A. Pais and S.B. Treiman, Phys. Rev. **D 12**, 2744 (1975).
[3] S.L. Glashow, J. Illiopolous, and L. Maiani, Phys. Rev. **D 2**, 1285 (1970).
[4] S. Eidelman *et al.* (Particle Data Group), Phys. Lett. B **592**, 1 (2004).
[5] M. Hosack, Fermilab–Thesis–2002–25.
[6] K. Abe *et al.* (Belle Collaboration), hep-ex/0408112.
[7] B. Aubert *et al.* (BABAR Collaboration), Phys.Rev. **D70** (2004) 091102.
[8] See the review on page 675 of S. Eidelman *et al.* (Particle Data Group Collaboration), Phys. Lett. B **592**, 1 (2004).
[9] T.S. Hill, Nucl. Instrum. Methods Phys. Res. A **418**, 32 (1998); D. Peterson, Nucl. Phys. **B** (Proc. Suppl.) **54B**, 31 (1997).
[10] Y. Kubota *et al.*, Nucl. Instrum. Methods Phys. Res. A **320**, 66 (1992).
[11] P. Billior, Nucl. Instrum. Methods Phys. Res., Sect. A **255**, 352 (1984).
[12] R. Brun *et al.*, GEANT3 Users Guide, CERN DD/EE/84-1.
[13] C. Sedlack, Ph.D. Thesis, University of Illinois, Urbana (2004).
[14] S. McGee, Ph.D. Thesis, Wayne State University, Detroit (2002).